

APPROACH FOR SIZING AND TURNDOWN ANALYSIS OF A VARIABLE GEOMETRY SPACECRAFT RADIATOR

Lisa Erickson and Andrew Loveless
NASA Johnson Space Center

ABSTRACT

Over the past few years, NASA has funded the development of several prototype radiator designs which use shape memory alloys to actuate cylindrical panels in response to changes in temperature. By adjusting each panel's view to space, variable geometry radiators aim to improve the variable heat rejection capabilities of future manned vehicles in a consumable free manner. A system level radiator model can help evaluate developing panel designs, but is difficult to construct due to the large number of panels that compose a radiator, as well as the parasitic heating of the panels. This paper describes a method for modeling a vehicle-sized variable geometry radiator using Thermal Desktop (with SINDA FLUINT). It exploits the Dynamic SINDA feature in combination with custom subroutines to piece together a string of steady-state solutions into a solution for the entire radiator. Only a small portion of the panels need to be physically present in the model. We demonstrate how this approach can be used to determine the size and minimum operational heat load of an example radiator configuration. Predicted radiator sizes are shown to be consistent with hand calculations using known fin efficiencies and sink temperatures.

INTRODUCTION

Single loop Active Thermal Control Systems (ATCSs) are viewed as an attractive means to reduce mass and complexity over traditional dual loop solutions. However, designing a single loop system suitable for manned spacecraft has been a longstanding technical challenge at NASA. Early trade studies for Orion determined that a single loop system was not capable of meeting the vehicle's heat rejection requirements [1]. Ochoa, Vonau, and Ewert concluded that when using traditional radiators, fluids safe enough to flow within crewed cabins cannot operate at temperatures low enough to survive the minimum heat load case. As a result, NASA has pursued several variable heat rejection radiator technologies intended to prevent the fluid from freezing at low temperatures. Recently, NASA has invested in the development of a variable geometry radiator that employs shape memory alloys (SMAs) to adjust the radiator's view to space. This technology is attractive because of its ability to adjust the heat rejected in a purely passive manner.

The radiator consists of multiple panels – each having a naturally closed cylindrical shape to reduce heat rejection for low vehicle heat load cases. SMAs integrated into each panel are tailored such that their temperature-dependent phase changes will cause the panels to gradually open to a semi-circular shape. Fundamentally, the radiator's heat rejection is adjusted by 1) the panels' changing views to space, and 2) the contrasting infrared spectrum emissivities, ϵ_{IR} , on

each side of the panels (i.e. convex side has a high ϵ_{IR} , concave side has a low ϵ_{IR}).¹ The radiator's operational concept is depicted in Figure 1. Radiation shields at the ends of each path help minimize heat rejection when closed. Short panels are required to prevent temperature gradients along a panel's length from causing it to open unevenly. Several prototype composite panels have been developed at Texas A&M – each 3in long with a 3in closed diameter.² Numerous laboratory tests, as well as several thermal vacuum tests conducted at JSC, have demonstrated their ability to successfully actuate [2].

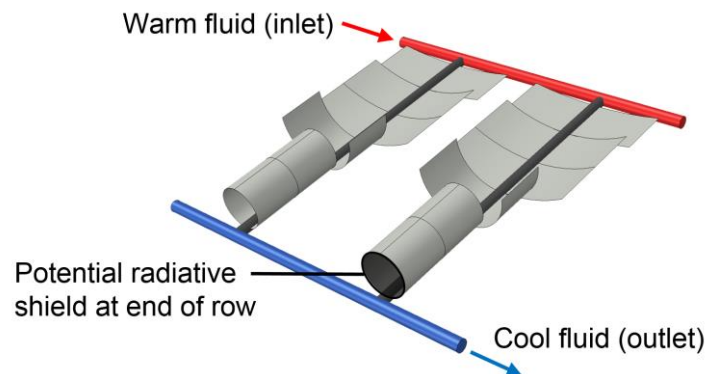


Figure 1: Conceptual fluid path layout for a variable geometry radiator.

Previously, a joint study conducted by Jacobs, Texas A&M, and NASA showed the potential benefits of morphing radiators to manned spacecraft [3]. Their analysis relied on commonly used environmental sink temperatures and did not account for the opening and closing of different radiator panels along a flow path. A higher fidelity thermal model was needed to evaluate the variable heat rejection potential of radiator designs currently in development. The steady-state sizing and heat rejection calculations used for traditional body mounted radiators cannot easily be applied to this technology. The complex radiation exchange of the curved panels, which results in parasitic heating of the radiator, is better characterized with a Monte Carlo method in a finite difference model. However, using geometric representations of hundreds of small panels to model a spacecraft's entire radiator would be tedious and error prone. This paper describes an alternative approach for steady-state modeling a variable geometry radiator in Thermal Desktop (with SINDA FLUENT).

Specifically, we make the following contributions:

- We describe a method for modeling a variable geometry radiator which actuates in response to changes in temperature. This method predicts heat rejection for an entire radiator using only the geometric representation of a small radiator segment (“Modeling Approach”).

¹ This concept assumes both sides of the panel have a low solar absorptance.

² Current development is focused on the panel's composite structure. Methods of controlling the panel's optical properties have not yet been investigated in detail.

- We show how the model's output can be used to size a radiator capable of rejecting a vehicle's maximum heat load ("Radiator Sizing").
- We show how the model's output can be used to determine the minimum operational heat load for a given radiator design ("Identifying Minimum Heat Load").
- We demonstrate that the model-based radiator sizing approach, applied to both flat and curved panels, produces results consistent with hand calculations using known fin efficiencies and sink temperatures ("Model Checking").

THE PROBLEM

Often first cut radiator sizing calculations are performed using basic steady-state heat transfer equations. For radiators with simple geometries (e.g. cylindrical body mounted), it is not difficult to calculate heat rejection by hand in programs like Excel and MATLAB. The heat rejected to space, Q , from a single radiator element, i , can be calculated using the following equation:

$$Q_i = \eta A_i \varepsilon \sigma (T_{root,i}^4 - T_{\infty,i}^4) \quad (1)$$

Here η denotes the radiator's fin efficiency, ε the radiator's emissivity in the infrared spectrum, σ the Stefan-Boltzmann constant, A_i the element's surface area, $T_{root,i}$ the element's base temperature, and $T_{\infty,i}$ the element's effective sink temperature [4]. Element i extends from the radiator panel's root to its fin tip. A fin ends either at the panel's edge or halfway between parallel fluid lines on the same panel. If the fin efficiency is given with respect to the radiator's working fluid, the fluid temperature at the element's root, $T_{fluid,i}$, replaces $T_{root,i}$ in Equation 1.

The sink temperature is used to simplify the energy balance equation by accounting for heat absorbed from the environment [4]. It is the temperature that the segment would reach at steady-state with no heat load (i.e. the adiabatic surface temperature), and is found by taking an energy balance over the element (Equation 2) [5]. Let α denote terms related to the solar spectrum, IR terms related to the IR spectrum, and q a heat flux per area. Equation 2 makes the common assumption that the radiator's surface is effectively gray in both the solar and IR spectrums. Therefore, α equals the absorptivity/emissivity in the solar band, and ε the absorptivity/emissivity in the IR band.

$$T_{\infty,i} = \sqrt[4]{\frac{1}{\sigma} \left(\frac{\alpha}{\varepsilon} q_{sol,i} + q_{IR,i} \right)} \quad (2)$$

The incident solar flux $q_{sol,i}$, on a flat surface i tilted at an angle θ_i from the sun, is calculated using Equation 3 – where G_{sun} is the solar constant [6].

$$q_{sol,i} = \cos(\theta_i) G_{sun} \quad (3)$$

The incident flux from bodies emitting in the infrared spectrum is:

$$q_{IR,i} = \varepsilon_i A_i \sigma \sum_{j=1}^n \varepsilon_j B_{ij} T_j^4 \quad (4)$$

where each radiation exchange factor B_{ij} could be replaced by a view factor F_{ij} if reflection off of other components is negligible [7]. For a cylindrical vehicle with body mounted radiators and no incident infrared radiation, Equation 2 resolves to Equation 5. A body mounted radiator's backside is generally well insulated from the vehicle, so heat transferred between them can be neglected in initial sizing calculations. Therefore, assuming $q_{IR,i} = 0$ is reasonable as long as the radiator does not view nearby vehicle components or planetary bodies.

$$T_{\infty,i} = \sqrt[4]{\frac{\cos(\theta_i) \alpha G_{sun}}{\varepsilon \sigma}} \quad (5)$$

The average sink temperature is found with Equation 6 [5].

$$T_{\infty,avg} = \sqrt[4]{\frac{\sum_{i=1}^n T_{\infty,i}^4}{n}} \quad (6)$$

First order radiator sizing calculations consider the entire radiator as a single element, and solve Equation 1 for area using the average sink temperature and average radiator fluid temperature. Commonly, the average sink temperature, root temperature, and heat rejection used correspond to the maximum heat load scenario.

When modeling the variable geometry radiator, the $q_{IR,i}$ term cannot be assumed zero nor easily calculated due to each curved panel's view to itself and adjacent panels. Moreover, panels may be open different amounts along a radiator's path. Thermal Desktop is well suited for modeling this behavior because of its ability to characterize the temperature gradient along a panel, as well as calculate the radiation exchange factors between panels. Each panel can be represented as a combination of many finite difference elements (with one node per element). The element temperatures can be predicted using SINDA/FLUINT, and the radiation exchange factors calculated using Monte Carlo methods in RadCAD.

RadCAD requires elements to be physically represented in Thermal Desktop [8]. This creates a challenge for modeling, since a typically sized radiator could contain thousands of panels. Such models would be exceedingly complex and inflexible to use in practice. Performing a sizing analysis would require additional panels to be physically modeled in each run until the correct radiator size was identified. Moreover, this entire process would need to be repeated if the radiator's parameters were changed (e.g. varying optical properties, space between panels, panel opening/closing temperatures).

The 2013 joint NASA, Texas A&M, and Paragon study that initially investigated the feasibility of the technology sidestepped this problem by modeling the radiator with one long panel (1.2m). The radiator's total heat rejection was calculated by multiplying the heat rejected from that panel by the number of paths comprising the entire radiator [3]. However, the single panel approach could not 1) open and close panels or 2) vary the space between panels along a path.

MODELING APPROACH

Using the proposed approach, the Thermal Desktop model need only contain a single reasonably sized radiator segment. The segment is constructed from a small number of panels and partial fluid paths. Custom subroutines utilizing Dynamic SINDA calculate the segment's steady-state solution, stringing the results together over successive runs to calculate the heat rejected over a full radiator path. The angle between the segment and the sun is increased incrementally from 0° to 180° for each new path. The results from all paths are used to determine the total heat rejected by the radiator. The number of panels along a radiator path, and therefore the length of the path, is adjustable at compile time. Moreover, both the distance between panels in a path and the distance between adjacent paths can be controlled by changing the values of predefined symbols. Because only steady-state solutions are calculated, thermal mass can be ignored. The following assumptions were made when constructing the model:

1. The radiator has an unobstructed view to space (i.e. no incident infrared radiation).
2. The radiator is body mounted to a cylindrical vehicle.
3. The radiator is well insulated from the vehicle (i.e. no conduction paths between them).
4. The fluid paths are straight, evenly spaced, and run along the length of the vehicle.
5. Flow is distributed evenly among the radiator paths.
6. The radiator includes circular radiation shields at the ends of each path.³

PHYSICAL STRUCTURE

The radiator segment is constructed entirely from primitive Thermal Desktop and FloCAD objects. Panels can be represented either with `solid cylinders` or `thin shells` [8]. The model currently uses `thin shells`, and therefore assumes no temperature gradient over the thickness of a panel. The use of `thin shells` also reduces run times, since fewer total nodes are needed in the model. Each panel is comprised of 150 elements – a number determined by increasing the element density until steady-state solutions for a single radiator path became nearly constant. An odd number of elements were placed along each panel's width. This allows the root temperature of each panel (i.e. the temperature directly above the radiator tube) to be recorded. Each path in the segment is comprised of 1) an `inlet plenum` (to provide an infinite fluid supply), 2) a `setflow` path to provide a constant flow rate, 3) a `pipe` to represent the flow tube, and 4) an `outlet plenum` to provide an infinite fluid sink. All `pipes` contain fluid

³ The 2013 analysis predicted that adding shields would prevent freezing at cooler inlet temperatures [3].

paths and linear conductors. The conductors add convection heat transfer between the fluid and the pipe wall [8].

The radiator segment in the model contains an odd number of paths – each containing an odd number of panels. The outlet temperature and heat rejection are calculated for the segment’s center panel. The number and arrangement of panels is intended to reproduce the effect that all surrounding panels in the radiator have on any given panel. As such, the heat transfer to/from the center panel in the model should be approximately the same as if the entire radiator was present.

Three preliminary models were constructed to assess the impact that adjacent paths have on the outlet temperature of the center path, and to therefore determine the minimum number of paths needed in the model. Each model contained only one panel per path – 1) 1 path, 1 panel, 2) 3 paths, 3 panels, and 3) 5 paths, 5 panels. Successive runs over each panel were used to characterize the fluid temperature along a full radiator path (which contains many panels). The outlet temperature calculated for each panel was used as the inlet temperature for the next panel in the path. Only outlet temperatures along the center path were recorded. The following cases were used to compare the three models:

Table 1: Key parameters for cases used to compare path arrangement in models.

	Flow Rate (lbm/hr)	ϵ (shields)	α (shields)	ϵ (panel concave)	α (panel concave)	ϵ (panel convex)	α (panel convex)
Case 1	0.25	0.03	0.14	0.75	0.75	0.345	0.345
Case 2	0.68	0.91	0.29	0.83	0.15	0.04	0.14

The optical properties for Case 1 assume the shields are polished aluminum, each panel’s concave side is bare composite, and each panel’s convex side is painted with LO/MIT-I paint. Case 2 assumes the shields are covered in Beta cloth, each panel’s concave side has the same optical properties as Optical Solar Reflectors (OSRs), and each panel’s convex side is covered with aluminized mylar. In all three models, the panels remained open for the duration of the run, the edges of adjacent panels were separated by 0.25in, and a single-phase 60/40 propylene glycol-water mixture was used. If the fluid’s boiling or freezing points were exceeded, properties for its maximum or minimum liquid temperatures were used.

Figure 2 shows the fluid temperatures along the center path in the three models. A different plot is given for each case. A lower path outlet temperature indicates that more heat was rejected. The difference between the single and multi-path models is minimal for paths facing either the sun or deep space. The difference is even more negligible in Case 2, since the low infrared emissivity on the outside of the panels means the paths are better insulated from each other. However, the single path model cannot account for shading from panels in adjacent paths – predicting warmer temperatures for the path tilted 90° from the sun. The outlet temperatures for the 3 and 5 path models are very similar for both cases and at all angles. These results indicated

that further increasing the number of panels would have little effect on the outlet temperature. The radiator segment in the model was therefore constructed with 3 paths.

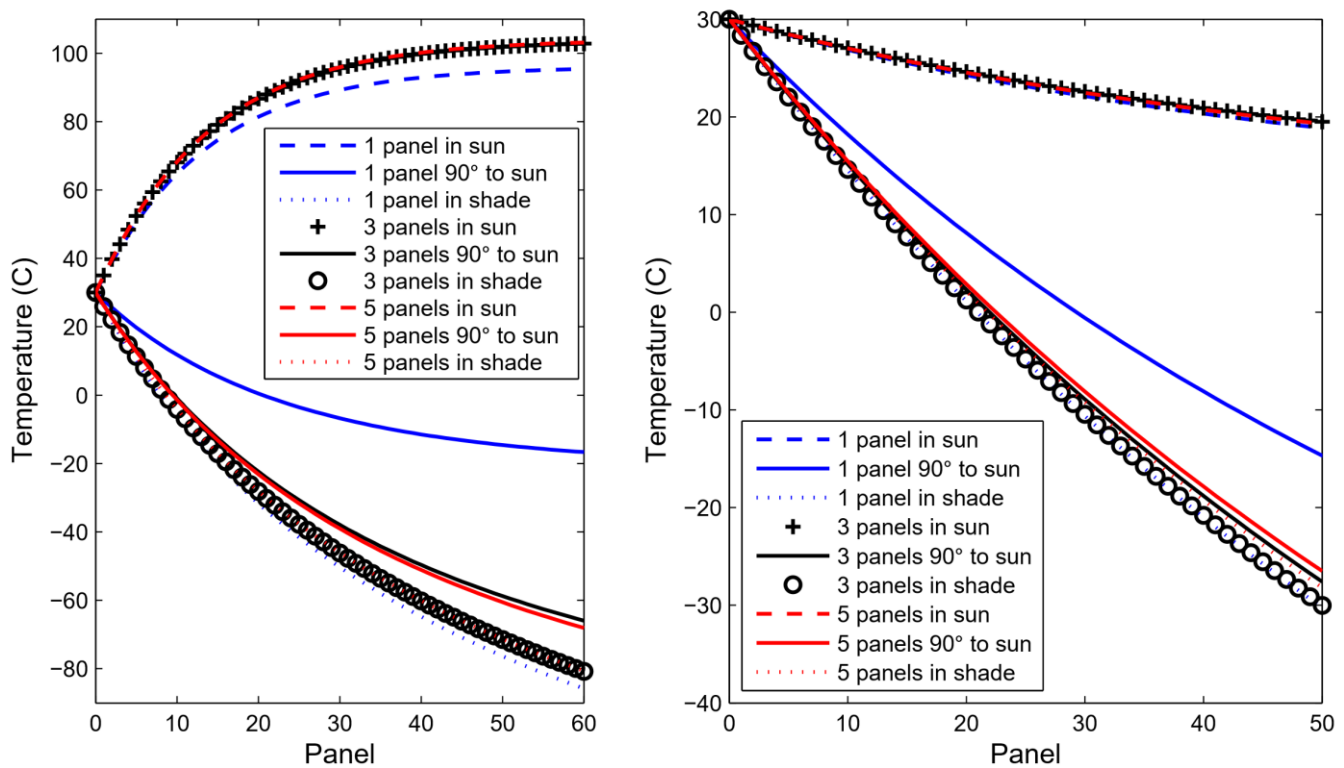


Figure 2: Panel outlet temperatures for paths at different locations around a cylindrical vehicle. Case 1 is on the left, and Case 2 is on the right.

Additional tests were performed to determine the minimum number of panels needed in each path. The first test compared the radiation conducted between the center panel and the other panels to that between the center panel and all modeled components (e.g. space, the vehicle). Conductances were calculated for a segment containing 3 paths of 9 panels each. Panels were separated by 0.25in – both along a path and between adjacent paths. The segment was oriented directly facing the sun, and the modeling parameters from Case 2 were used. All panels were also closed, since closed panels in the same path have greater radiation exchange with one another than open panels in the same path. Figure 3 shows the radiation conductances from the center panel to its surrounding panels as a percentage of its total conductance to the entire model. The largest percentages are for the panels directly preceding and following the center panel in the same path. The conductances to panels in neighboring paths are extremely low. The asymmetry in conductances in the figure is due to error in calculating the radiation exchange factors. Increasing the number of rays used in the Monte Carlo simulation (from 5,000 to 50,000) reduces the asymmetry, while also reducing the conductance to panels in neighboring paths.

This analysis indicated that the conductance from the center panel to the panels on the ends of each path (i.e. panels 1 and 9) accounted for only 0.74% of its total conductance. From these

results, it was determined that the radiator segment in the model needed to contain only 7 panels per path. A second test was performed to verify this conclusion. The fluid temperatures along a path were calculated for both the 3 paths, 7 panels and 3 paths, 9 panels cases. Again the modeling parameters from Case 2 were used. The models were configured to close any panel whose root temperature fell below -10C. Figure 4 shows the fluid temperatures along the center path in the two models. In both configurations, the temperatures were determined to closely agree. These results supported the previous conclusion that only 7 panels per path were needed in the model.

0.005	0.35	0.006
0.001	1.1	0.01
0.055	4.8	0.053
0.039	31.8	0.035
0.056		0.059
0.034	31.77	0.037
0.051	4.72	0.05
0.007	1.04	0.013
0.008	0.36	0.007

Figure 3: Percentages of the total radiation conductance from the center panel to the other panels in the segment.

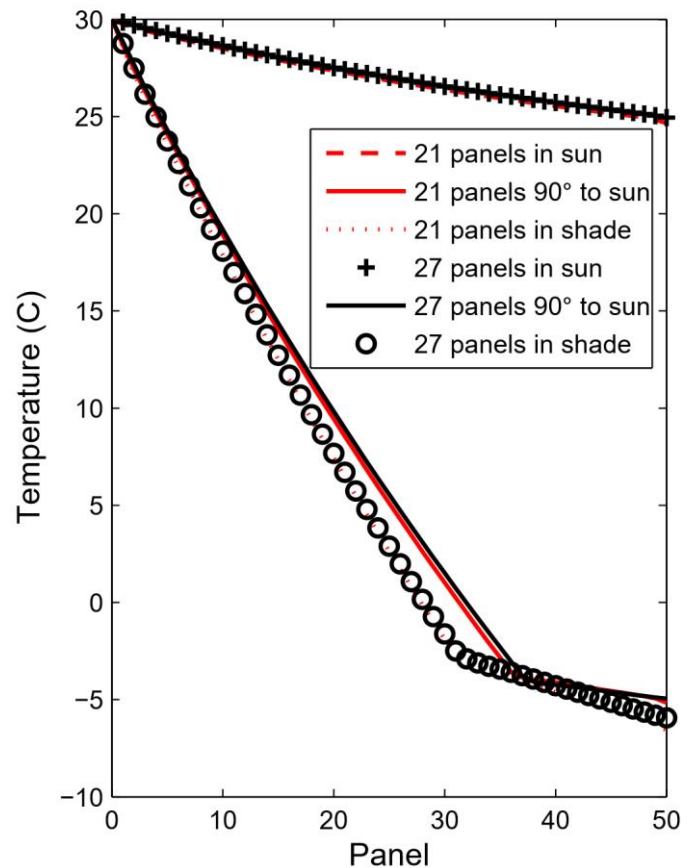


Figure 4: Comparison of fluid temperatures at different locations around a cylindrical vehicle for the 21 and 27 panel models.

The radiator segment is pictured in Figure 5. The vehicle surface is modeled using three finite difference rectangles – each 0.04in thick and made of stainless steel. The purpose of modeling the surface is to account for the 1) vehicle shading panels from the sun, and 2) radiation exchange between the panels and the vehicle. One rectangle is placed underneath each of the paths. The rectangles on either side are angled depending on the configured distance between adjacent paths – approximating a curved surface. The paths are likewise angled to match the surface to which they are mounted. Generally a vehicle's surface is well insulated from the cabin environment. A radiation conductor with an effective

emittance ϵ^* of 0.032 is used to represent this insulation – connecting each rectangle to a 20C cabin temperature boundary node.

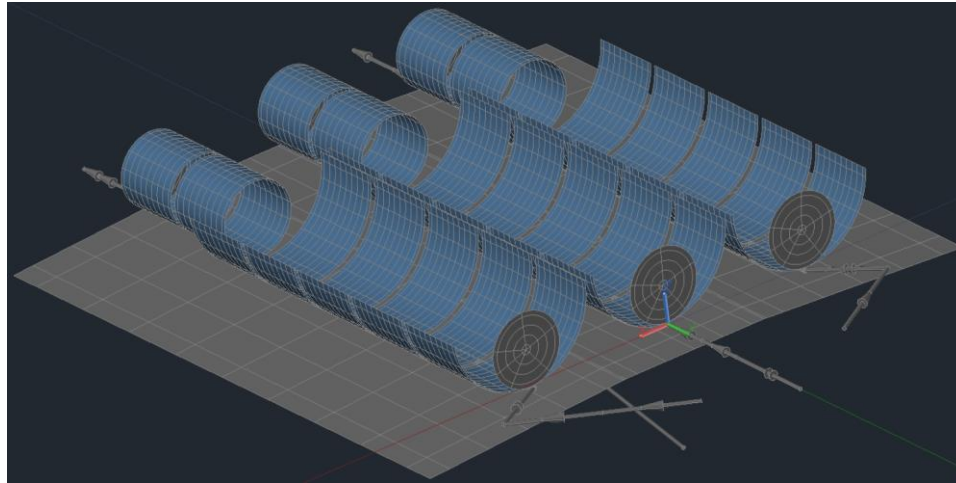


Figure 5: Radiator segment containing 3 paths of 7 panels each.

Incident solar flux is added using a static `orbit` with no albedo. To verify the `orbit` was setup properly, a `1in × 1in` rectangular coupon with an emissivity of 1 was placed above the vehicle (prior to modeling the radiator segment). Only the side of the coupon facing the sun participated in the radiation calculations, and its view to space was unobstructed. The direct absorbed heat flux on the coupon was found by post-processing calculated heat rates and verified to match the desired flux from the sun. `X` and `Y orbit` rotations are used to adjust both the vehicle's angle to the sun (e.g. side to sun, tail to sun) and the placement of the radiator segment around the vehicle's circumference (0 to 180°).

Radiation shields are modeled as `disks` at the ends of each path. They only reflect rays in the radiation exchange calculations – i.e. their surfaces are set to `Active=NONE` in the model's radiation analysis group [8]. If the shields could absorb energy from the sun, they would heat up and provide an inaccurately warm radiator environment for cold vehicle orientations. To quantify this effect, average sink temperatures were calculated for the center panel using the method outlined in the Appendix. Again panels were spaced 0.25in apart and the modeling parameters from Case 2 were used. Figure 6 shows the average sink temperatures calculated for the center panel for cases where the panels are either open or closed, facing or not facing the sun, and with shields absorbing or not absorbing energy. For fully shaded open panels, allowing the shields to absorb energy results in a 129K increase in average panel sink temperature. Moreover, Figure 6 shows that modeling the shields to not absorb energy has little impact on the sink temperatures of panels facing the sun. Assuming the shields do not absorb energy biases the panels at the ends of the paths to be colder. This cold bias is acceptable, however, since it increases the likelihood of the fluid freezing at the coldest vehicle orientation (i.e. it makes the worst case more severe).

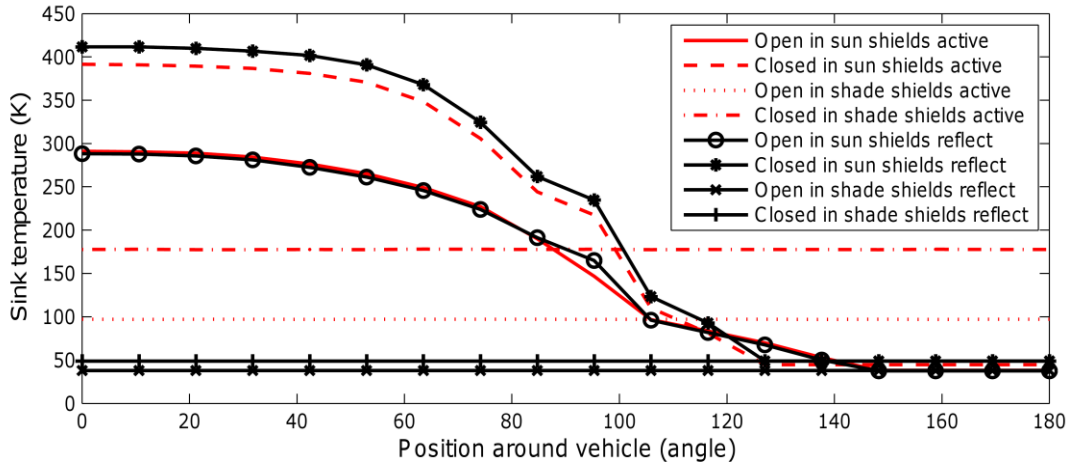


Figure 6: Comparison of average panel sink temperatures. Active denotes shields both absorbing and emitting radiation. Reflect denotes shields only reflecting rays.

LOGIC

The model's process for calculating the heat rejected by the panels, as well as their fluid outlet temperatures, is automated using custom FORTRAN subroutines.⁴ As a result, running the model requires the user to execute only a single case in the Case Set Manager. The top level subroutine is called within the case's Operations Block to start the solution process. All custom subroutines are located in a single logic object in the Logic Object Manager. The key subroutines can be summarized as follows:

Table 2: Key subroutines used for predicting the radiator's steady-state behavior.

<code>calc_all()</code>	<ul style="list-style-type: none"> Sets the radiator's mass flow rate, inlet temperature, and vehicle orientation (e.g. side to sun, tail to sun). Calls <code>calc_rad()</code> to execute one case. Calls <code>calc_flows()</code> or <code>calc_tins()</code> to execute multiple cases.
<code>calc_flows()</code>	<ul style="list-style-type: none"> Calls <code>calc_rad()</code> or <code>calc_tins()</code> in a loop varying the radiator's flow rate.
<code>calc_tins()</code>	<ul style="list-style-type: none"> Calls <code>calc_rad()</code> in a loop varying the radiator's inlet temperature.
<code>calc_rad()</code>	<ul style="list-style-type: none"> Calls <code>calc_path()</code> in a loop varying the segment's angle to the sun.
<code>calc_path()</code>	<ul style="list-style-type: none"> Calls <code>calc_panel()</code> in a loop moving the segment along the path's length.
<code>calc_panel()</code>	<ul style="list-style-type: none"> Calls SINDA's <code>STEADY</code> subroutine to obtain the segment's steady-state solution [9].

The segment's angle to the sun maps to the path's location around the vehicle and is set by changing the `orbit's` Y rotation (from 90°, full sun to 180°, full shade). `calc_path()` is called $M/2$ times, where M is the total of number paths around the vehicle. Because both the vehicle and radiator are symmetric, only half of the paths need to be solved (the other half are

⁴ This model was created using Thermal Desktop Version 5.8.

identical). For each path, the following are written to an output file: 1) the path's angle around the vehicle, 2) its total heat rejection, and 3) its outlet temperature. `calc_panel()` is called K times, where $K = \text{Panels per Path} - (\text{Segment Length in Panels} - 1)$. A 50 panel long path would therefore require 44 calls to `calc_panel()`. For each panel, the following values are recorded: 1) fluid outlet temperature, 2) heat rejected, 3) root temperature, and 4) degree to which the panel is open.

The model obtains steady-state solutions for the entire segment, but only records results (e.g. outlet temperature) for specific panels in the segment's center path. Because of edge effects at the ends of each path, the first/last 3 panels in the center path of the segment can only be used to represent the first/last 3 panels in a full path. The middle panel represents any panel along the path besides the first/last 3 panels. Therefore, assuming a 7 panel long segment, processing an N panel long path requires the following operations:

1. Obtain results for panels 1 to 4: `calc_panel()` records results of first 4 panels in the segment's center path.
2. Obtain results for middle N-8 panels: `calc_panel()` records results of segment's middle panel. Perform operation N-8 times.
3. Obtain results for last 4 panels: `calc_panel()` records results of last 4 panels in the segment's center path.

To string the solutions together, calculations for panels 5 to N must have knowledge of the previous panels' states. After obtaining results for panels 1 to 4 (i.e. after the initial `calc_panel()` call), the segment effectively 'moves' down the length of the path by first saving for each path in the segment: 1) the 2nd to 4th panels' temperatures and open/close angles, and 2) the 1st panels' fluid outlet temperatures. For the next calculation, the previous segment's 2nd to 4th panels' results are used as boundary conditions for the current segment's 1st to 3rd panels. Moreover, the previous 1st panels' outlet temperatures are used as the fluid inlets for the current segment's 1st panels. This process is illustrated in Figure 7 for the first two calls `calc_path()` makes to `calc_panel()`.

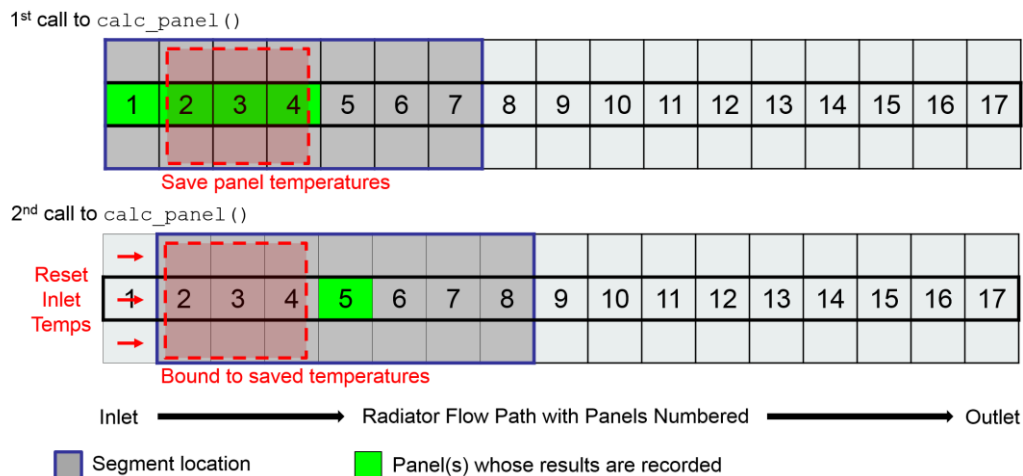


Figure 7: Process of stringing steady-state solutions together to 'move' segment along a radiator path.

Again the purpose of the segment's outer two paths is to provide a realistic radiation environment for the center path. This is why their temperatures and open/closed states are also updated when stringing the solutions together. The heat rejected by a panel is obtained after a call to STEADY by calling SINDA's QFLOWSET and QFLOW subroutines. These determine the heat transferred from the segment's middle pipe to the panel. Since QFLOW does not allow the panel's nodes to be boundary nodes, the ADDMOD and DRPMOD subroutines are used to convert from boundary to diffusion nodes and back [9].

By default, when SINDA calculates successive solutions as a part of a single case in the Case Set Manager, results from the previous solution are overwritten in memory [8, 9]. To avoid this, results are recorded in high level subroutines and used to initialize successive runs. Others, such as node temperatures, are written to output files and read the next time the subroutines which use them are called.

Panels are either open or closed. A panel closes if its predecessor's root temperature falls below a specified threshold. To model this behavior, if one of the first 4 panel's in a path falls below the threshold, then the first call to `calc_panel` will update the geometry and re-calculate the solution before recording results. Otherwise, if a panel's root temperature is calculated to be below the threshold, then the geometry is updated before the next call to `calc_panel`.

Thermal Desktop must recalculate radiation exchange factors each time the segment's geometry changes. For this to occur, the Dynamic SINDA feature is enabled in the Case Set Manager prior to running the model. Subroutines use the following process to update the model's geometry when changes are necessary (e.g. closing a panel, changing the angle to the sun): 1) set the corresponding registers, 2) call TDSETREG or TDSETREGINT to update Thermal Desktop on the register changes, 3) call TDUPDATE to physically update the segment's geometry, and 4) call TDCASE to recalculate the radiation exchange factors [8]. Geometric updates can be monitored using the Dynamic SINDA status window. Accessing particular SINDA and Thermal Desktop functionality by calling COMMON is not required. However, subroutines which set the fluid's flow rate and calculate stead-state solutions must call COMMON [9]. It's important to note that because Dynamic SINDA is used, the model cannot run multiple cases in parallel [8].

SIZING & TURNDOWN CALCULATIONS

The model was used to size a radiator and predict its minimum operational heat load in the coldest vehicle orientation for an example configuration. The radiator was assumed to be a part of a single loop ATCS, shown in Figure 8, with both an internal and a radiator bypass line. The radiator bypass helps maintain the cabin heat exchanger inlet set point, while the internal bypass helps prevent condensation on the cold plates. Commonly, dynamic heat loads from the cold plates and cabin heat exchanger drive the amount of flow required through the internal bypass line. To simplify calculations, however, a linear approximation based on reference [10] was used to determine the fraction of total vehicle flow entering the radiator and its bypass. At full load, 80% of the total mass flow was diverted towards the radiator. At $\frac{1}{4}$ of the full load, 40% of the total mass flow was sent to the radiator and its bypass.

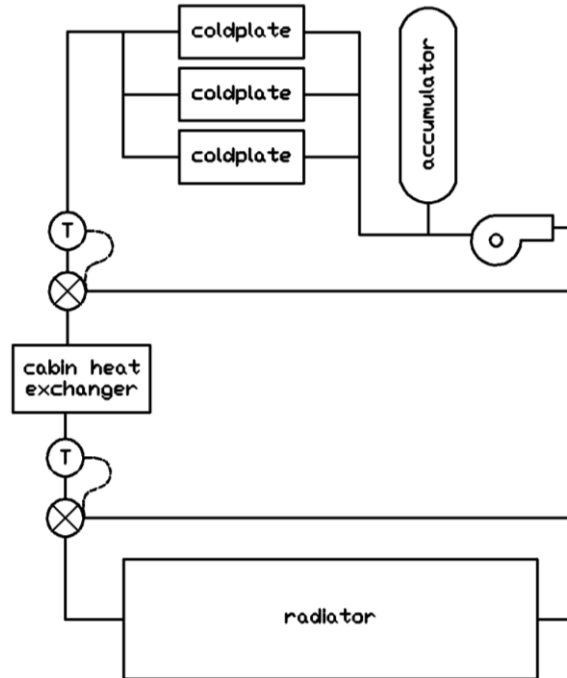


Figure 8: Thermal control system for radiator sizing and turndown calculations.

The following key parameters describe the rest of the example configuration:

- Vehicle size: Length: 5m, Diameter: 5.5m
- Vehicle surface: $\varepsilon = 0.03$, $\alpha = 0.2$ (3M-425 aluminized tape)
- Environment: 0K
- Solar flux: 1414W/m^2
- Max heat load: 8kW
- Hottest orientation: Side to sun (one path is in full sun)
- Coldest orientation: Tail to sun (all paths see deep space)
- Working fluid: 60/40 propylene glycol-water mixture
- Radiator inlet during full load: 30C
- Minimum radiator inlet: 16C
- Cabin heat exchanger inlet set point: 4C
- Minimum allowable fluid temperature: -16C (5C margin from -21C freeze point)
- Maximum allowable pressure drop: 3psi at full load
- Number of radiator paths: 100
- Space between panels along a path: 0.25in
- Radiator panel size: Width: 3in, Length: 4.71in, Thickness: 0.0175in
- Panel concave side: $\varepsilon = 0.83$, $\alpha = 0.15$ (OSRs)
- Panel convex side: $\varepsilon = 0.04$, $\alpha = 0.14$ (aluminized mylar)
- Panel thermal conductivity: 238W/mK (based on [2])
- Panel full open threshold temperature: 4C (180° angle, semi-circle)

- Panel full closed threshold temperature: -10C (359.4° angle)
- Flow tube material: Aluminum
- Flow tube size: Outer diameter: 0.1875in, Inner diameter: 0.1575in
- Flow tube does not participate in radiation calculations.
- Radiation shields: Aluminum disks
- Radiation shields optics: $\epsilon = 0.91$, $\alpha = 0.29$ (simulating a beta cloth covering)
- Shield to tube contact: 0.1in thick epoxy with a thermal conductivity of 7.5W/mK and a contact area of 0.125in by 0.04in.

RADIATOR SIZING

The first step of the sizing process is to calculate the mass flow rate, \dot{m} , required by the maximum heat load case (assuming no flow through the radiator bypass line). This is done with Equation 7, where cp_{fluid} stands for the specific heat of the fluid.

$$\dot{m} = \frac{Q}{cp_{fluid}(T_{rad\ inlet} - T_{cabin\ inlet})} = \frac{8000}{3591.2(30 - 4)} = 0.00856 \frac{kg}{s} \rightarrow 680 \frac{lbm}{hr} \quad (7)$$

Next, the model is run in the hottest vehicle orientation using that flow rate. Here an upper bound for the radiator length must be provided. For this example, 50 panels was used. The model outputs text files containing each panel's fluid outlet temperature, heat rejected, base temperature, and angle. Below is a snippet from the output file for the first path:

Panel #,	Tin,	Qout,	Panel_angle,	Tbase
0,	30.0000,	0.0000,	180.0000,	0.0000
1,	29.7536,	0.5696,	180.0000,	27.7453
2,	29.5720,	0.5221,	180.0000,	28.1561
3,	29.4231,	0.4603,	180.0000,	28.1974
4,	29.2821,	0.4331,	180.0000,	28.1211

Output data is read into MATLAB and used to calculate the total heat rejection and outlet temperatures for radiators of different lengths (1 to 50 panels here). The path length needed to reject 8kW and have an outlet temperature of 4C is identified and automatically marked in a plot, shown in Figure 9. The vertical lines indicate that 44 panels are sufficient for the maximum heat load case. The bends in the curves are due to closing of panels in a portion of the paths (since closed panels reject less heat). The fluid then is verified to not fall below its minimum allowable temperature of -16C. Figure 10 shows the temperature gradient along each of the 50 fluid paths. The warmest line corresponds to the path directly facing the sun, while the coldest lines correspond to paths that only view deep space. From the plot, the minimum fluid temperature is shown to be roughly -6C. Lastly, the Darcy-Weisback equation is used to verify that the pressure drop through the coldest path in this case is <3psi.

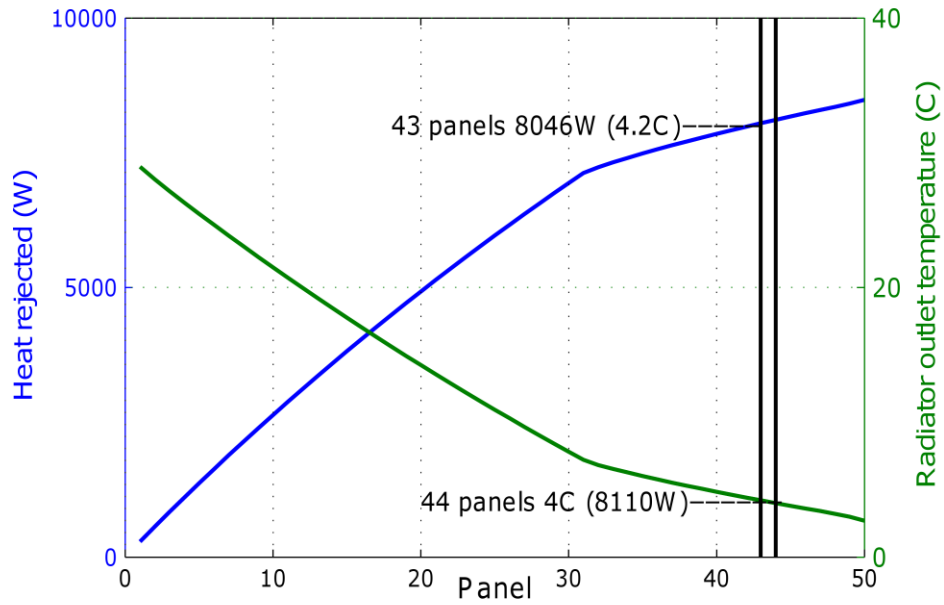


Figure 9: Model results for the full load case. The black lines mark the number of panels required per path to meet the radiator's requirements.

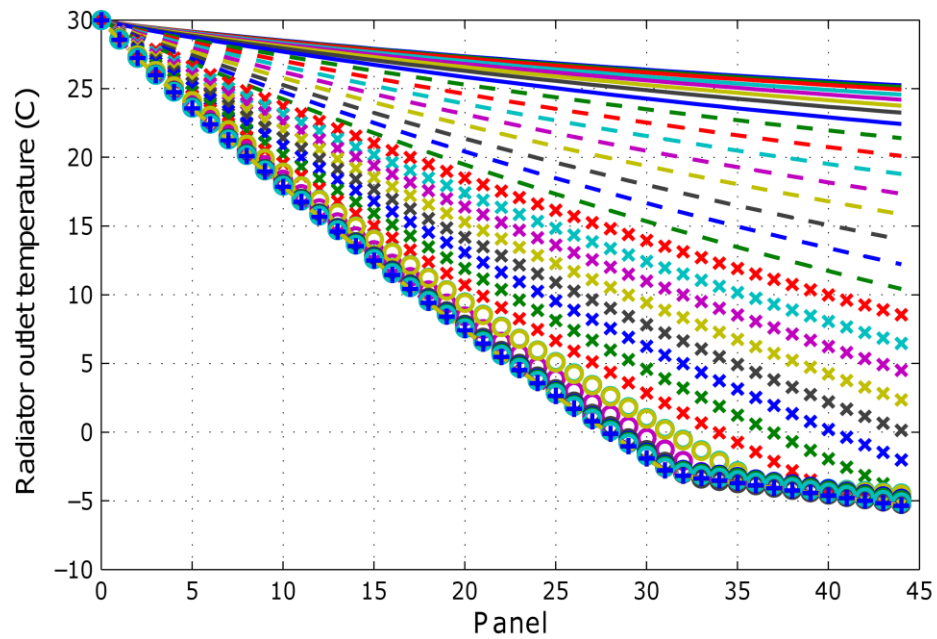


Figure 10: Panel outlet temperatures for each path under the full heat load.

IDENTIFYING MINIMUM HEAT LOAD

To determine the minimum operational heat load in the coldest vehicle orientation, the radiator's steady-state behavior is predicted over a range of flow rates and inlet temperatures. Here cases are run with flow rates from 320lbm/hr to 480lbm/hr (in 10lbm/hr increments) with radiator inlets from 30C to 16C (in 2C increments). Since all paths have the same environment, they are identical and thus only one path needs to be solved (i.e. `calc_path()` only needs to be called once). The total heat rejected by the vehicle in this case is the heat rejected by one path \times 100. In each case, the total heat rejected by the vehicle is used to determine the total flow diverted towards the radiator and its bypass with the linear approximation from [10]. Then a mass average is used to determine the mixed radiator and bypass outlet temperature (i.e. the cabin heat exchanger inlet). In MATLAB the cabin heat exchanger inlet, total heat rejection, minimum fluid temperature, and percent of panels which are open are found for each case. These results are interpolated and plotted in Figure 11. Cases are removed that violate either the minimum allowable fluid temperature ($<-16\text{C}$) or the specified cabin heat exchanger inlet temperature range ($<3\text{C}$ or $>7\text{C}$).

The minimum operating condition for a 3.4C cabin heat exchanger set point is: 26.5C radiator inlet, 5.71kW rejected, 320lbm/hr through the radiator, -13.3C radiator outlet, and 231lbm/hr through the radiator bypass. At this state 35% of the panels are still open. The example configuration is not quite able to operate at half its total heat load. When reading these results, it's important to understand that they only reflect the performance of the example radiator. Performance can be significantly improved by 1) decreasing the distance between panels along a path (limiting the concave side of a closed panel's view to space), and 2) decreasing the absorptivity of the panel's convex surface (to reduce heat absorbed by closed panels in the sun). Modeling the gradual opening and closing of the panels may also affect performance.

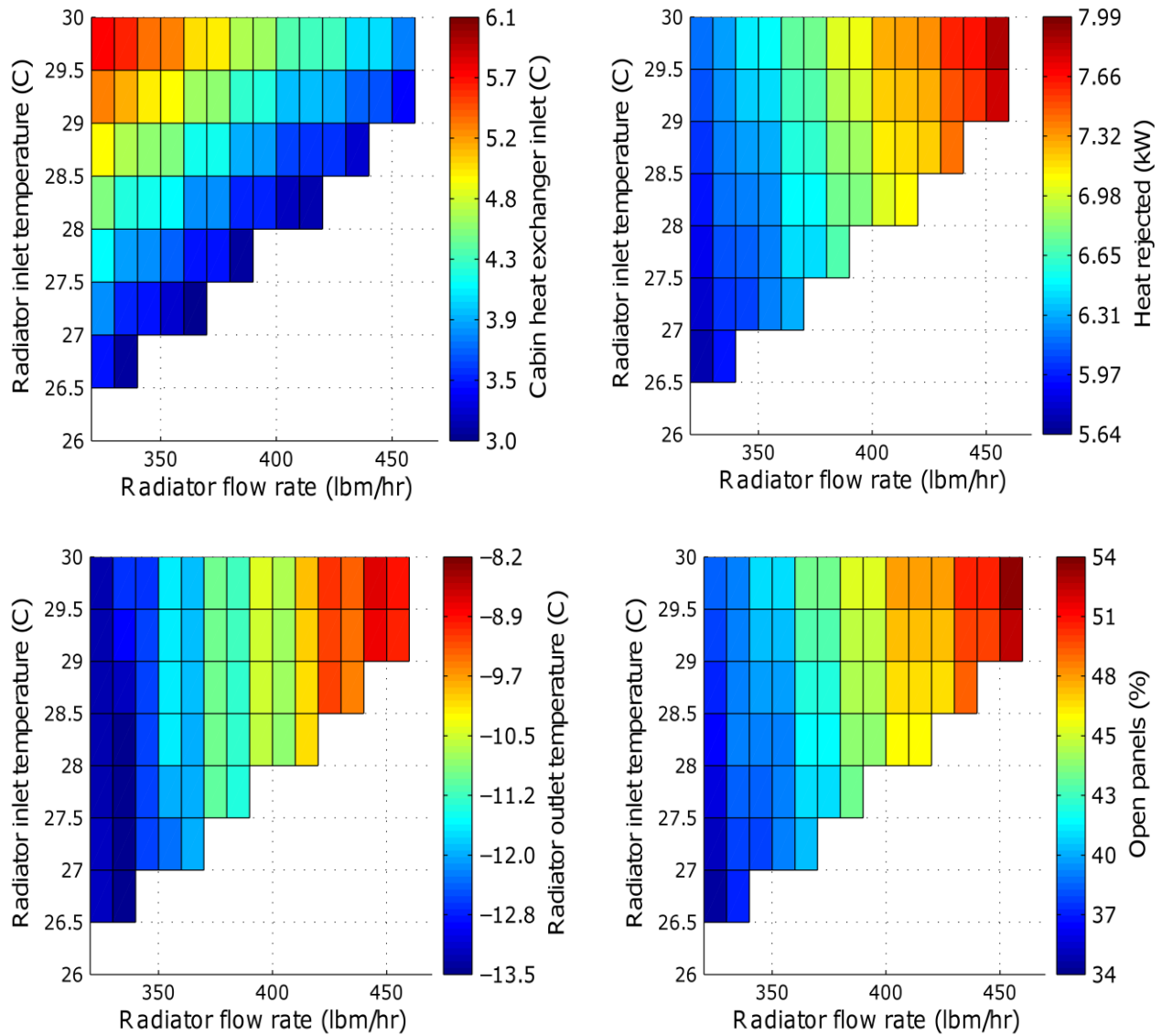


Figure 11: Mixed outlet temperature of radiator and bypass loop (top left), total radiator heat rejection (top right), minimum radiator temperature (bottom left), and percent of open panels (bottom right) for example case.

MODEL CHECKING

To verify the accuracy of the model, it was used to size both a flat radiator and a radiator with statically open curved panels. The results were then compared to those obtained from traditional sizing calculations (Equations 1-6) using fin efficiencies calculated from the model's output. Radiator sizing hand calculations were performed in Excel using the same parameters as the above example. The flat radiator was assumed to consist of 3in \times 6in, 0.25in thick aluminum panels (shown in Figure 12).

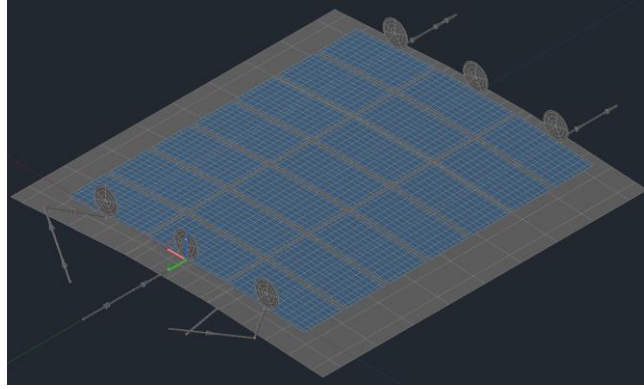


Figure 12: Radiator segment with flat panels.

Equations 5 and 6 were used to calculate the radiator's average sink temperature in the hottest vehicle orientation (side to sun). For the curved radiator, the average sink temperature was calculated using Thermal Desktop with the method outlined in the Appendix. Fin efficiencies needed for sizing the radiator were obtained using Equations 8 and 9. For both the flat and curved radiators, the actual heat rejection per panel, $Q_{p,actual}$, and average fluid temperature, $T_{fluid,avg}$, was predicted by the model for a string of panels in a path facing deep space. The projected area, A_p , was found by multiplying the total projected area of a single panel (3in \times 6in) by the number of panels in the string.

$$\eta = \frac{Q_{actual}}{Q_{ideal}} = \frac{\sum_{p=1}^{ptot} Q_{p,actual}}{Q_{ideal}} \quad (8)$$

$$Q_{ideal} = \varepsilon \sigma A_p (T_{fluid,avg}^4 - T_{\infty,avg}^4) \quad (9)$$

Table 3 displays the results of the comparison:

Table 3: Comparison of hand radiator sizing calculations to model predictions.

Type	$A_{p,shade}$ (m^2)	$T_{\infty,shade}$ (K)	$T_{fluid,avg}$ (K)	Q_{ideal} (W)	Q_{actual} (W)	η	$T_{\infty,avg}$ (K)	A_p (m^2)	N_{panels} (hand)	N_{panels} (model)
Flat	0.372	0.0	289.9	123.5	104.3	0.844	195.0	35.9	30.8	31
Curved	0.372	38.0	289.7	123.2	103.3	0.838	224.0	44.4	38.2	37

The seemingly low fin efficiencies were a result of the laminar flow within the tube, which leads to a noticeable difference in fluid and root temperatures. As expected, using the average root temperature for the flat panel (274K) instead of the average fluid temperature produced a fin efficiency of 1. For both cases, the number of required panels predicted using the model and using Equations 1-6 were nearly identical.

SUMMARY/CONCLUSIONS

A system level model was needed to evaluate and compare different variable geometry radiator designs. We presented a method for modeling the radiator which requires only a small radiator segment to be physically modeled in Thermal Desktop. A model was shown that can be used to 1) perform a steady-state radiator sizing analysis and 2) predict its steady-state minimum operational heat load. The model is easily configurable, allowing changes to the space between panels and the number of panels along a radiator path. The segment size used may not be suitable for all configurations but can be easily adjusted. The use of open FloCAD loops limits the model's applicability to steady-state cases. A different method will need to be developed to model transient behavior. Additionally, the model is limited to representing parallel radiator paths. The model's accuracy could be improved by including the ability to partially open and close panels.

ACKNOWLEDGEMENTS

The authors would like to acknowledge Texas A&M for their great work on the development of a variable geometry radiator. We would also like to thank Hee Song for reviewing this paper and Christopher Bertagne for providing the radiator concept image used in Figure 1.

CONTACT

Lisa Erickson
Thermal Systems Branch (EC6)
NASA Johnson Space Center
lisa.erickson@nasa.gov

NOMENCLATURE

ATCS	Active Thermal Control System
θ	Angle
A	Area
ε	Emissivity
η	Fin efficiency
q	Heat flux
Q	Heat rejection
\dot{m}	Mass flow rate
n	Number

OSR	Optical Solar Reflector
A_p	Projected area
B_{ij}	Radiation exchange factor
SMA	Shape Memory Alloy
∞	Sink
G_{sun}	Solar constant
cp	Specific heat
σ	Stefan-Boltzmann constant
T	Temperature

REFERENCES

- [1] D. A. Ochoa, W. Vonau, and M. K. Ewert, "A Comparison between One- and Two-Loop ATCS Architectures Proposed for CEV," 01-Jan-2009.
- [2] C. L. Bertagne, J. B. Chong, J. D. Whitcomb, D. J. Hartl, and L. R. Erickson, "Experimental Characterization of a Composite Morphing Radiator Prototype in a Relevant Thermal Environment," presented at the AIAA SCITech 2017, Grapevine, TX, United States, 2017.
- [3] T. J. Cognata, D. Hardtl, and C. Dinsmore, "A Morphing Radiator for High-Turndown Thermal Control of Crewed Space Exploration Vehicles," presented at the SciTech 2015, Kissimmee, FL, United States, 2015.
- [4] D. G. Gilmore, *Spacecraft Thermal Control Handbook*, 2nd ed. El Segundo, Calif.: Reston, Va.: Aerospace Press; American Institute of Aeronautics and Astronautics, 2002.
- [5] E. K. Ungar, "Slat Heater Boxes for Control of Thermal Environments in Thermal/Vacuum Testing," 1999.
- [6] F. P. Incropera, T. L. Bergman, and A. S. Lavine, *Introduction to Heat Transfer*, 5th ed. New York: John Wiley & Sons, 2007.
- [7] J. R. Howell, *Thermal Radiation Heat Transfer, 5th Edition*, 5th ed. Boca Roca: CRC Press, 2010.
- [8] Timothy D. Panczak, Steven G. Ring, Mark J. Welch, David Johnson, Brent A. Cullimore, and Douglas P. Bell, "Thermal Desktop A CAD Based System for Thermal Analysis and Design User's Manual Version 5.8." C&R Technologies, Inc. ("CRTech"), 2015.
- [9] Brent A. Cullimore, Steven G. Ring, and David Johnson, "SINDA/FLUINT General Purpose Thermal/Fluid Network Analyzer User's Manual Version 5.8." C&R Technologies, Inc. ("CRTech"), 2015.
- [10] Ungar, Eugene K. and K. Jentung, "Actively Controlled Loop Heat Pipes as a Human Spacecraft External Active Thermal Control System." 2017-ICES-210, 46th International Conference on Environmental Systems, 16-Jul-2017.

APPENDIX – CALCULATING SINK TEMPERATURES

Two methods were used to calculate average sink temperatures of panels in each radiator path. The first method fakes the ability to apply no heat load to the radiator by running the model with a very low flow rate (e.g. 0.01kg/hr per path). Therefore, along the path's length, panels slowly approach their adiabatic surface temperatures. Once this occurs, the fluid will reach a constant temperature – approximating the sink temperatures for all panels in the path. For this method, panels are set either statically open or closed. Since many paths have sink temperatures below the fluid's freezing point, fluid properties are limited to their minimum liquid values.

In the second method, a custom subroutine calls SINDA's `TSINK1` in a loop to calculate sink temperatures for each node in the segment's middle panel [9]. An average sink temperature is then calculated for the panel using Equation 6. This result is assumed to be the same for all other panels in the radiator path where the middle panel is located. To automatically calculate sink temperature in different paths, the segment's angle to the sun is adjusted using Dynamic SINDA. For this method to produce correct results, the model's fluid components must be disabled [8]. As opposed to the first method, which calculates many steady-state solutions per path, this approach only requires calculating one solution per path. Therefore, it produces results much faster (on the order of ~15 minutes verses a few hours).

Results from both methods were compared for a case using 1) Case 2's parameters from the "Physical Structure" subsection, 2) open panels, and 3) a side to sun vehicle orientation. The first method flowed 0.01kg/hr through each path. The second method calculated sink temperatures every 10 degrees around the vehicle. Figure 13 shows panel sink temperatures at different locations around the vehicle's circumference. While these results are not identical, they produce nearly identical average vehicle sink temperatures. A vehicle sink of 224.2K was produced with the first method and 223.9K with the second method.

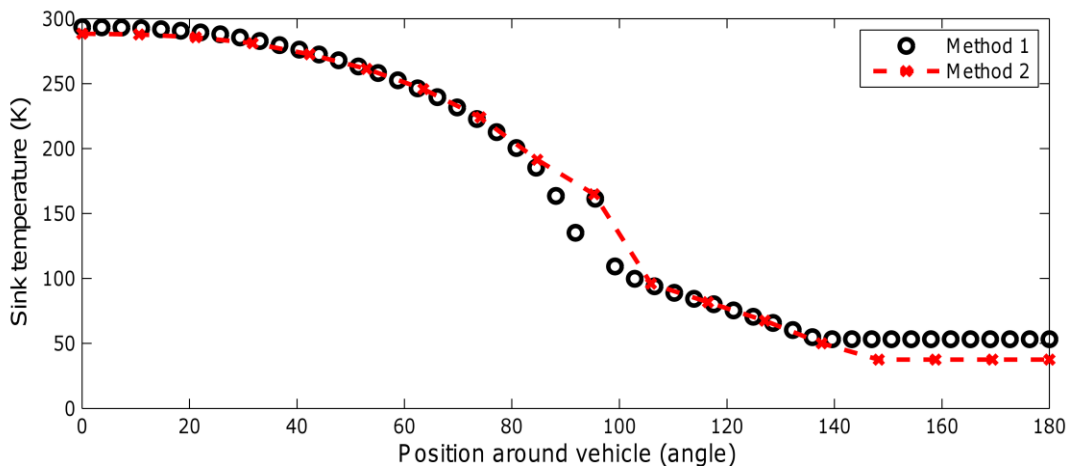


Figure 13: Panel sink temperatures predicted for a vehicle with its side to the sun.